Progress In Electromagnetics Research Letters, Vol. 61, 13–18, 2016

Orbital Angular Momentum Radiation from Circular Patches

Fuchun Mao[1, *], Tinghua Li[2], Yu Shao[1], Jianfeng Yang[1], and Ming Huang[1]

Abstract—Orbital angular momentum (OAM) with a huge potential application in multiplexing and coding has become the subject of intense research in recent years. This paper presents a method to generate radio beams carrying OAM based on a circular patch antenna. A 3 dB quadrature hybrid is employed in the design to enable the circular patch to reconfigure opposite OAM states of a radiated field. The results of numerical simulations are presented to show that the circular patch radiates two OAM modes with opposite rotation directions simultaneously. The proposed circular patch is believed to be significant to the wireless communication applications due to its simple geometry, low cost, and OAM mode reconfiguration.

1. INTRODUCTION

With the rapid development of mobile internet, user data are explosively increased, which puts much higher requirements on the capacity and spectrum efficiency of communication systems. By providing much more transmission channels on a limited spectrum band, the technologies of multiplexing greatly improve both the capacity and spectrum efficiency of the communication system. OAM is an external parameter to describe the transverse rotating characteristics of electromagnetic waves. What is important is that the different OAM modes are orthogonal to each other, thus the channels identified by different OAM states can be clearly distinguished from each other. Such a property of OAM makes it possible to be used in multiplexing [1]. At present, by applying the OAM multiplexing, the communication system has been able to achieve data rate at least $320\,\mathrm{Tb{\cdot}s^{-1}}$ and spectrum efficiency $230\,\mathrm{Tb{\cdot}s^{-1}{\cdot}Hz^{-1}}$, which is much higher than LTE system's [2, 3].

As the basis of developing the OAM multiplexing technology, simple and efficient methods for generating OAM beams have been the hot spot in academic attention in recent years [4–6]. In an optical band or even in Terahertz regime, the OAM generation can be achieved easily by multiple methods such as spiral plate [7], metasurface [8], q-palate [9], computer-generated holograms [10], whispering gallery modes based emitter [11], Dammann optical vortex grating [12], anisotropic dielectric plate [13], spiral plasmonic lens [14], chiral polaritonic lenses [15, 16], etc. However, in microwave regime, the selectable recipes for OAM generation are still rare. The phased circular antenna array was investigated to generate OAM beams [17–20]. Nevertheless, the complexity of this scheme is too high to implement in many scenarios. Helical paraboloid antenna was presented in [21] to radiate OAM carried beams, while its OAM mode was not reconfigurable, and a paraboloid reflector assisting OAM generator was employed in the pending patent [22] to enhance propagation performance. Recently, both circular traveling-wave antenna [23, 24] and circular polarized patch antenna [25] were demonstrated to produce OAM beams. In this paper, we propose an antenna that combines the circular patch and 3 dB quadrature hybrid to generate radio beams with good defined OAM mode, and the signs of OAM mode are reconfigurable.

Received 26 January 2016, Accepted 27 May 2016, Scheduled 7 June 2016

* Corresponding author: Fuchun Mao (22014000162@mail.ynu.edu.cn).

[1] Wireless Innovation Lab of Yunnan University, School of Information Science and Engineering, Kunming, Yunnan 650091, China.

[2] Technical Center of China Tobacco Yunnan Industrial Co., Ltd., Kunming 650231, China.

2. MODEL OF THE ANTENNA

A model of a circular patch is shown in Figure 1, where Figure 1(a) shows the full view of the antenna, Figure 1(b) the top view, and Figure 1(c) the bottom view. It is clear from Figure 1(a) that the infrastructure of antenna is composed of circular patch '1', feed network '2' and substrate '5'. The feed network is electrically connected with a metallic patch through vias ① and ②. The ground plane is set at the middle of the substrate. The vias and ground are electrically isolated, which is guaranteed by isolation belts set at the ground plane, i.e., '3' and '4' presented in Figure 1(a). '6' and '7' are the input ports of excitations, which can be excited individually or simultaneously. It is noteworthy that the feed network adopted here is a 3 dB quadrature hybrid. So the signal from the output of via ① will delay -90 degrees than that from via ②, when the input port of '6' is individually excited, and vice versa. This provides the circular patch the ability of OAM modes reconfiguration, i.e., l and $-l$, where l is the mode number of OAM. The radius of metallic circular patch is a, and its relationship with the resonance frequency f_r can be expressed as [26]

$$f_r = \chi_{nm} c/(2\pi a\sqrt{\varepsilon_r}) \tag{1}$$

where χ_{nm} is the nth root of $J'(\cdot) = 0$ and $J'(\cdot)$ the derivative of Bessel function of the first kind. For the antennas whose working frequency is greater than 2 GHz, a in formula (1) must be substituted by an equivalent radius a_e, which can be calculated as bellow [27]

$$a_e = a\left[1 + 2h(\ln(\pi a/2h) + 1.7726)/(\pi a\varepsilon_r)\right]^{1/2} \tag{2}$$

where h is the thickness of substrate. According to the theory of cavity, the z-component of electric field in thin cylindrical cavity can be expressed as

$$E_z = E_0 J_n\left(k_{nm}\rho\right)\cos n\varphi \tag{3}$$

where $J_n(\cdot)$ is the first kind of Bessel function, $k_{nm} = \chi_{nm}/a$ the wavenumber of resonance modes TM_{nm}, and ρ the radial distance. The distributions of electric field intensity are shown in Figure 2, where l is the index of TM_{n1} mode, which is also equal to the mode number of OAM in our case.

It is demonstrated vividly in Figure 2 that surface electric fields close to the periphery of circular patches are enhanced remarkably and alternately. The number of such enhanced local distributions of surface electric field is equal to $2n$, which can be considered as the element of a circular antenna array. Thereout, it may be inferred that radiation from circular patch resonating at TM_{n1} mode behaves as a circular array with $2n$ elements, which can reconfigure all the OAM states with mode number $-n < l < n$. Managing to rotate the local enhanced fields clockwise or anticlockwise, the radio beams carrying OAM can be radiated. One approach is to use dual feed ports, i.e., the 1st and 2nd ports

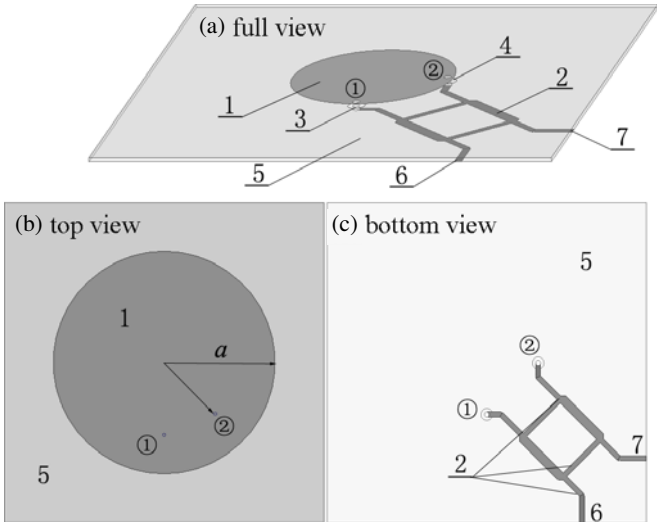

Figure 1. The structure diagram of proposed circular patch.

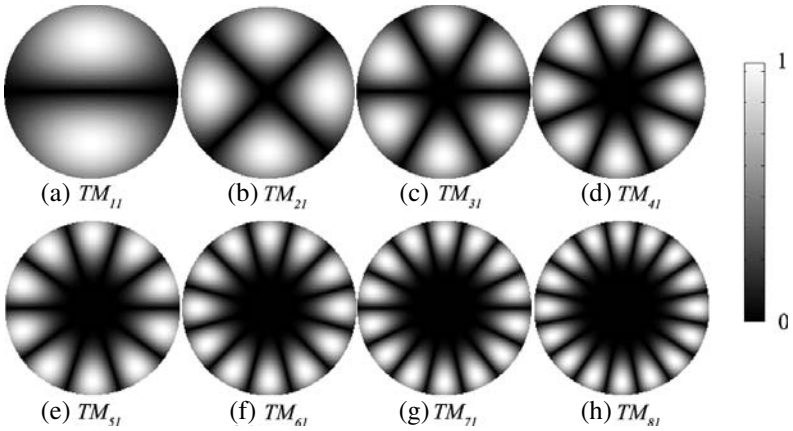

Figure 2. Normalized distributions of surface electric field for circular patches operate at TM_{n1} modes.

excite TM_{n1} mode respectively, then making the two TM_{n1} modes to be mutually orthogonal. After this arrangement, the surface current will operate under travelling wave state, and OAM beams will be radiated naturally. Concretely, the proposed circular patch applies a 3 dB quadrature hybrid network to achieve the objective, which has already been shown in Figure 1(c).

3. RESULTS AND DISCUSSIONS

Assuming that the working frequency is 2 GHz, the thickness and dielectric constant of an FR4 substrate are 0.762 mm and 4.6, respectively. As mentioned above, χ_{nm} is the root of $J'(\cdot) = 0$. So for the resonant modes TM_{11}, TM_{21} and TM_{31}, χ_{nm} is equal to 1.84118, 3.054 and 4.201 in turn. According to formula (1), the radii of circular patches working at TM_{11}, TM_{21} and TM_{31} modes can be calculated as 20.4934 mm, 34.2 mm and 46.76 mm, respectively. These designs are performed by the commercial electromagnetic simulation software HFSS.

Figure 3 presents the normalized distributions of surface electric fields for antennas, in turn, working at TM_{11}, TM_{21} and TM_{31} modes, where ① and ② represent vias electrically connected to the feed network printed on the opposite surface of the substrate, which is a 3 dB quadrature hybrid circuit. The positions of ① and ② are separated by an angular distance of $(2k+1)\cdot 90°/l$, where k is integer by principle; however, we set k=0 in our case for concise concern. It is obvious that the simulated results on surface electric field distribution shown in Figure 3 agree well with those computed results shown in Figure 2(a) to Figure 2(c). Moreover, the local enhanced electric fields presented in Figure 3 are rotational over time, which leads to the OAM radiation.

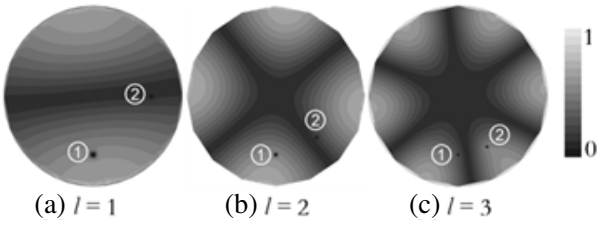

Figure 3. Normalized surface electric field distribution of designed circular patches operating at OAM modes $l = 1$, $l = 2$ and $l = 3$ in turn.

Figure 4 shows the normalized transverse electric field intensity distributions of helical beams carrying OAM with mode number $l = 1$, $l = 2$ and $l = 3$ in turn. Obviously, all the radiated electromagnetic fields possess the characteristics of helix. For the beams with mode number $|l| > 1$, the distributions of their fields at transverse plane are hollow, and the size of such a hollow center

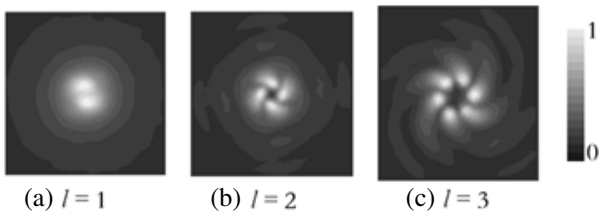

Figure 4. Normalized electric field intensity distribution of radio beams with OAM mode number $l = 1$, $l = 2$ and $l = 3$ in turn.

cell extends with the larger mode number. For the beam with OAM modes $|l| = 1$, they degenerate into right-handed (or left-handed) circularly polarized field, thus there are no hollows in their boresight propagation.

Figure 5 presents the phase structure of E_z radiated from antennas, which work at the resonant modes TM_{11}, TM_{21} and TM_{31} in turn. It is observed that spiral orbits with good defined number appear in the wave fronts of the radiated fields. Such spiral phase distributions are the most important characteristics of OAM beams. In other words, helical beams with clearly defined OAM states can be achieved by the proposed circular patch based microstrip antenna.

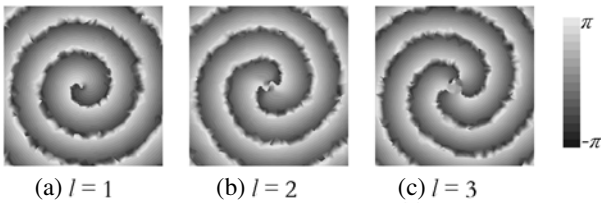

Figure 5. Phase structure of E_z fields with OAM mode number $l = 1$, $l = 2$ and $l = 3$ in turn.

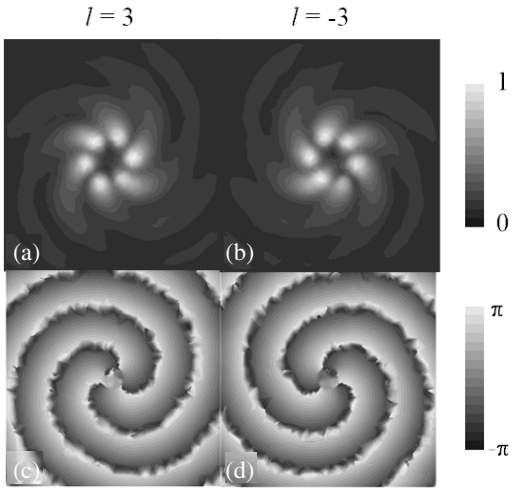

Figure 6. The distributions of electric field intensity and phase of radiated field, where circular patch works at mode $l = 3$ and $l = -3$ respectively.

Figure 6 demonstrates the reconfiguration of OAM states with mode number $l = 3$ and $l = -3$, where Figure 6(a) and Figure 6(b) are the distributions of phase and electric field for the mode $l = 3$, respectively, and Figure 6(c) and Figure 6(d) for the mode $l = -3$. In the case of Figure 6(a) and Figure 6(b), we only excite port '6', while in the case of Figure 6(c) and Figure 6(d), we only excite port '7'. The inverse spiral features are observed both in the phase structure and electric fields, which shows

that by selecting the excited port at will, the proposed antenna can reconfigure dual OAM modes with opposite signs.

4. CONCLUSIONS

A combination of a circular patch and 3 dB quadrature hybrid circuit is proposed to construct the circular patch to reconfigure helical beams with opposite OAM states. The operating principle and radiation characteristics of the circular patch are discussed in detail. Moreover, multiple numerical examples are demonstrated particularly to verify the validity of the proposed circular patches. The proposed circular patches are beneficial to the wireless communication due to their simple geometry, easy manufacture, low cost, and reconfigurable mode.

ACKNOWLEDGMENT

This work was supported by the National Natural Science Foundation of China (Grant No. 61461052), the Specialized Research Fund for the Doctoral Program of Higher Education (Grant No. 20135301110003), the Seventh of Yunnan University Graduate Student Scientific Research Project (Grant No. ynuy201443), and the doctoral award for the academic newcomers (2014) of Yunnan Province.

REFERENCES

1. Willner, A. E., H. Huang, Y. Yan, et al., "Optical communications using orbital angular momentum beams," *Advances in Optics and Photonics*, Vol. 7, No. 1, 66–106, 2015.
2. Wang, J., S. Li, C. Li, et al., "Ultra-high 230-bit/s/Hz spectral efficiency using OFDM/OQAM 64-QAM signals over pol-muxed 22 orbital angular momentum (OAM) modes," *Optical Fiber Communication Conference, Optical Society of America*, W1H, 4, San Francisco, USA, 2014.
3. Parkvall, S., A. Furuskär, and E. Dahlman, "Evolution of LTE toward IMT-advanced," *IEEE Communications Magazine*, Vol. 49, No. 2, 84–91, 2011.
4. Bozinovic, N., Y. Yue, Y. Ren, et al., "Terabit-scale orbital angular momentum mode division multiplexing in fibers," *Science*, Vol. 340, No. 6140, 1545–1548, 2013.
5. Wang, J., J. Y. Yang, I. M. Fazal, et al., "Terabit free-space data transmission employing orbital angular momentum multiplexing," *Nature Photonics*, Vol. 6, No. 7, 488–496, 2012.
6. Yao, A. M. and M. J. Padgett, "Orbital angular momentum: origins, behavior and applications," *Advances in Optics and Photonics*, Vol. 3, No. 2, 161–204, 2011.
7. Sueda, K., G. Miyaji, N. Miyanaga, et al., "Laguerre-Gaussian beam generated with a multilevel spiral phase plate for high intensity laser pulses," *Optics Express*, Vol. 12, No. 15, 3548–3553, 2004.
8. Karimi, E., S. A. Schulz, I. De Leon, et al., "Generating optical orbital angular momentum at visible wavelengths using a plasmonic metasurface," *Light: Science & Applications*, Vol. 3, No. 5, e167, 2014.
9. Slussarenko, S., A. Murauski, T. Du, et al., "Tunable liquid crystal q-plates with arbitrary topological charge," *Optics Express*, Vol. 19, No. 5, 4085–4090, 2011.
10. Heckenberg, N. R., R. McDuff, C. P. Smith, et al., "Generation of optical phase singularities by computer-generated holograms," *Optics Letters*, Vol. 17, No. 3, 221–223, 1992.
11. Cai, X., J. Wang, M. J. Strain, et al., "Integrated compact optical vortex beam emitters," *Science*, Vol. 338, No. 6105, 363–366, 2012.
12. Lei, T., M. Zhang, Y. Li, et al., "Massive individual orbital angular momentum channels for multiplexing enabled by Dammann gratings," *Light: Science & Applications*, Vol. 4, No. 3, e257, 2015.
13. Shu, W., D. Song, Z. Tang, et al., "Generation of optical beams with desirable orbital angular momenta by transformation media," *Physical Review A*, Vol. 85, No. 6, 063840, 2012.

14. Chen, W., D. C. Abeysinghe, R. L. Nelson, et al., "Experimental confirmation of miniature spiral plasmonic lens as a circular polarization analyzer," *Nano Letters*, Vol. 10, No. 6, 2075–2079, 2010.
15. Dall, R., M. D. Fraser, A. S. Desyatnikov, et al., "Creation of orbital angular momentum states with chiral polaritonic lenses," *Physical Review Letters*, Vol. 113, No. 20, 200404, 2014.
16. Yu, H., H. Zhang, Y. Wang, et al., "Optical orbital angular momentum conservation during the transfer process from plasmonic vortex lens to light," *Scientific Reports*, Vol. 3, 2013.
17. Thidé, B., H. Then, J. Sjöholm, et al., "Utilization of photon orbital angular momentum in the low-frequency radio domain," *Physical Review Letters*, Vol. 99, No. 8, 087701, 2007.
18. Mohammadi, S. M., L. K. S. Daldorff, J. E. S. Bergman, et al., "Orbital angular momentum in radio — a system study," *IEEE Transactions on Antennas and Propagation*, Vol. 58, No. 2, 565–572, 2010.
19. Sjöholm, J. and K. Palmer, "Angular momentum of electromagnetic radiation," UPTEC F07 56, 2007.
20. Mao, F., M. Huang, J. Zhang, et al., "Graphene assisted radiation adjustable OAM generator," *Progress In Electromagnetics Research M*, Vol. 42, 31–38, 2015.
21. Tamburini, F., E. Mari, A. Sponselli, et al., "Encoding many channels on the same frequency through radio vorticity: first experimental test," *New Journal of Physics*, Vol. 14, No. 3, 03300, 2012.
22. Mao, F., M. Huang, and J. J. Yang, *Patent Application Number in China*, 201410230978.7, 2014.
23. Zheng, S., X. Hui, X. Jin, et al., "Transmission characteristics of a twisted radio wave based on circular traveling-wave antenna," *IEEE Transactions on Antennas and Propagation*, Vol. 63, No. 4, 1530–1536, 2015.
24. Hui, X., S. Zheng, Y. Chen, et al., "Multiplexed millimeter wave communication with dual orbital angular momentum (OAM) mode antennas," *Scientific Reports*, Vol. 5, 2015.
25. Barbuto, M., F. Trotta, F. Bilotti, et al., "Circular polarized patch antenna generating orbital angular momentum," *Progress In Electromagnetics Research*, Vol. 148, 23–30, 2014.
26. Bahl, I. J. and P. Bhartia, *Microstrip Antennas*, Artech House, 1980.
27. Derneryd, A. G., "Analysis of the microstrip disk antenna element," *IEEE Transactions on Antennas & Propagation*, Vol. 27, No. 5, 660–664, 1977.